Erosional response to northward-propagating deformation in the coastal ranges of the Pacific Northwest

Andrew S. Gendaszek
Greg Balco
David R. Montgomery
John O. H. Stone
Nathaniel Thompson
Quaternary Research Center and Department of Earth & Space Sciences, University of Washington, Seattle, WA 98195-1310, USA

Keywords: Erosion, Coast Ranges, Cosmogenic Nuclides, Be-10, Relief

Abstract

We measured erosion rates in coastal drainage basins of the northwestern United States between the Columbia River and Cape Mendocino, CA, using cosmogenic ^{10}Be in riverborne quartz sediment. Erosion rates are near 0.3 mm/yr in the northern Oregon Coast Range, decrease to 0.1-0.2 mm/yr in the central Oregon Coast Range, and increase to 0.5-1.1 mm/yr in the northern California Coast Range. This distribution of erosion rates reflects the landscape response to northward-propagating crustal thickening and rock uplift associated with the Mendocino Triple Junction (MTJ). Erosion rates track uplift rates throughout the study area, suggesting a relatively short timescale for the erosional response to changes in uplift rate. The relationship between erosion rates and topographic relief changes with increasing erosion and uplift rates near the MTJ. This suggests that erosion rates respond to an increase in uplift rates through the development of threshold slopes preventing further increases in relief.

Introduction

The coastal ranges of the northwestern U.S. provide a unique setting to examine the timescale and magnitude of the erosional response to changes in uplift driven by the northward migration of the Mendocino Triple Junction (MTJ) at the southern terminus of the Cascadia Subduction Zone. Geodynamic models of deformation associated with the MTJ migration predict that a transient wave of rock uplift has propagated northward through the Northern California Coast Ranges during the last several million years at ~5 cm/yr, the speed of MTJ migration relative to the North American plate (Furlong and Govers, 1999). We measured erosion rates of drainage basins spanning the advancing limb of this transient uplift from the central Oregon Coast Range, where long-term uplift rates have not yet been affected by the advancing MTJ, to the Northern California Coast Ranges immediately overlying the MTJ at Cape Mendocino.

Study Area

The study area encompasses the coastal ranges between the Columbia River and Cape Mendocino, which include the Oregon Coast Range, the Klamath Mountains, and the Northern California Coast Ranges. Glaciation has been minimal in this area, and fluvial and hillslope processes are the primary agents of erosion. The Oregon Coast Range is composed mainly of siltstones and sandstones of the Eocene Tyee Formation (Dott and Bird, 1979), which started to emerge in the Miocene in response to syn-subduction uplift (McNeill et al., 2000). Summit elevations rarely exceed 500 m, and this region has the wettest climate in the study area, with annual rainfall approaching 3 m/yr. The Klamath Mountains include older, more competent meta-sedimentary and plutonic rocks of Paleozoic and Mesozoic age (Irwin, 1960) and are significantly higher than the Oregon Coast Range with average elevations approaching 1000 m. The Northern California Coast Ranges are composed of a diverse set of rock types of the Franciscan Complex, which include poorly consolidated mélange as well as more competent sandstone units (Blake et al., 1985). Total rainfall decreases and becomes more seasonal to the south, and the combination of steep slopes, mechanically weak lithologies, and infrequent, high-intensity storms in this region results in some of the highest sediment yields observed in the contiguous U.S. (Judson and Ritter, 1964; Brown and Ritter, 1971).

Methods

We collected sand from 16 coastal rivers (Figure 1; Table 1 in Data Repository), choosing sample sites in confined channels within bedrock valleys upstream of both tidal influence and extensive floodplains. Each sample was wet sieved to obtain sediment in the 0.25-0.5 mm grain size fraction. In addition, we sieved sediment in the Alsea River into two additional size fractions: 0.125-0.25 mm and 0.5-0.85 mm.

^{10}Be is produced in quartz by cosmic ray bombardment of rock and soil in the first few meters below the Earth's surface. Where the surface is eroding, the residence time of a mineral grain in this sub-surface production zone depends on the rate at which overlying material is removed. Therefore, the ^{10}Be concentration in river sediment is inversely related to the mean erosion rate in the upstream drainage basin. Mathematical formulae and the complete set of assumptions inherent in this method are discussed in detail elsewhere (Bierman and Nichols, 2004).

In calculating erosion rates, we accounted for ^{10}Be production by both spallation and muon reactions, using the scaling scheme of Stone (2000) for spallogenic production and the method of Heisinger et al. (2002a,b) for production by muons. Several earlier studies in the northwest coastal ranges area only accounted for spallogenic production (Bierman et al., 2001; Heimsath et al., 2001) underestimating erosion rates by 10 – 50% (Stone et al., 1998; Granger et al., 2001; Balco et al., 2008). We recalculated erosion rates from these studies to facilitate comparison to our data by accounting for both spallation and muon reactions.

Erosion Rates

Erosion rates are near 0.3 mm/yr in the northern Oregon Coast Range, decrease to a minimum of near 0.1 in the Siuslaw basin in the central Oregon Coast Range, and then increase to 0.5 - 1.1 mm/yr in the Northern California Coast Ranges inland of Cape Mendocino (Table 1 in Data Repository; Figure 1). These erosion rates are averaged over the ca. 600 – 6300 years necessary to erode the mean attenuation length of ^{10}Be production. Our results agree with several previously published cosmogenic ^{10}Be erosion rate measurements in the study area: 0.15-0.2 mm/yr at Drift Creek and Mettman Ridge in the central Oregon Coast Range (Bierman et al., 2001 and Heimsath et al., 2001) and 0.438 ± 0.088 mm/yr at Redwood Creek in the Northern California Coast Ranges (Ferrier et al., 2005). The ^{10}Be concentrations of quartz in varying grain sizes from the Alsea River agree within measurement uncertainty.

Erosion Rates Compared to Climate

Mean annual precipitation in the Coast Ranges decreases from nearly 3 m/yr in the northern Oregon Coast Range to 1 m/yr in the Northern California Coast Ranges (Figure 1). The average number of days of rainfall increases from 120 days in the Eel River watershed to 220 days in the northern Oregon Coast Range, thus suppressing latitudinal variation in rainfall intensity, an important control on the frequency of debris flows (Wilson et al. 1997). Erosion rates, on the other hand, are higher to the south. Neither total annual precipitation nor rainfall intensity are positively correlated with erosion rates, indicating that climate as measured by the modern distribution of mean annual precipitation and rainfall intensity is not the primary control on erosion rates in this region.

Erosion Rates Compared to Topography

Erosion rates grossly correlate with the elevation and local relief of the coastal ranges: the lowest erosion rates correspond to relatively low elevations and relief in the Oregon Coast Range, whereas the highest erosion rates are associated with the higher topography and relief of the Klamath Mountains and the Northern California Coast Ranges (Figure 2). Erosion rates approximately increase with local relief within the Oregon Coast Range and Klamath Mountains (Figure 2), in agreement with global compilations of basin-scale erosion rates that suggest relief exerts a strong control on erosion rates (Ahnert, 1970). In contrast, the Northern California Coast Ranges erosion rates vary widely among basins with similar local relief and exhibit no correlation, suggesting no dependence of the erosion rate on local relief similar to that thought to be characteristic of so-called ‘threshold landscapes.’ (Montgomery and Brandon, 2002).

The concept of a threshold landscape originated from observations of linear hillslope profiles in some landscapes (Penck, 1953), which suggest maintenance at a critical slope angle by landslides or other sediment transport processes whose rate is a strongly nonlinear function of slope. Erosion rates in a threshold landscape ought to be independent of slope angle and therefore of local relief. Such slopes respond to an increase in the uplift rate by an increase in the frequency of landsliding rather than an adjustment in slope and local relief (Montgomery and Brandon, 2002). Thus, a threshold landscape is expected to display a narrow range of local relief over a wide range of erosion rates, whereas a strong correlation is expected between erosion rate and local relief in a sub-threshold landscape. A number of studies (e.g., Burbank, 1996; Montgomery, 2001; Montgomery and Brandon, 2002; Binnie et al., 2007) have observed these two erosion rate-relief relationships in regional studies and global compilations; we suggest a similar effect here.

In the Oregon Coast Range, Montgomery (2001) showed that mean slope angle (and therefore local relief) is correlated with uplift rate; our measurements show that erosion rates are correlated with local relief. Both observations suggest that in this region, where erosion rates are relatively low, the balance between uplift and erosion rates is maintained by adjustments of slope angle and by a dependence of erosion rate on local slope. In contrast, the Northern California Coast Ranges display no relationship between erosion rate and local relief. This suggests that they have reached the critical value of local relief where changes in uplift rates can be balanced by changes in erosion rates without adjustment of slope and local relief. A key difference between the present data set and the global compilation of Montgomery and Brandon (2002) is that we observe decoupling between erosion rate and local relief at a much lower local relief than observed in the global data set (800 m vs. 1500 m). We attribute this to the relative mechanical weakness of the rocks in the Northern California Coast Ranges compared to rocks in other suggested threshold landscapes. If correct, this suggests a strong lithologic control on the critical relief in a landscape (e.g., Schmidt and Montgomery, 1995).

Erosion Rates Compared to Uplift Rates

Uplift rates averaged over ~10^4 year timescales can be inferred from the elevation of marine terraces that have been mapped along much of the northwest Coastal Ranges (Kelsey et al., 1994 and references therein; Merritts and Bull, 1989; McLaughlin et al., 1983) (Figure 1). Extraordinarily high uplift rates are recorded by terraces along the King Range in Northern California (ca. 4 mm/yr), but the King Range is tectonically decoupled from inland regions (Blake et al., 1985); therefore, the King Range terraces do not depict uplift in our study basins and we disregard these data in the remainder of the discussion. In the Oregon Coast Range, uplift rates inferred from marine terraces are as high as 0.8 mm/yr at a few sites near major coastline-normal faults, but overall suggest regional uplift rates of ~0.1 mm/yr in the central Oregon Coast Range and ~0.2-0.3 mm/yr in the southern Oregon Coast Range (Figure 1). At the southern end of our study area south of Cape Mendocino, uplift rates inferred from marine terraces are 0.3-1.2 mm/yr (Figure 1).

Outside of the King Range, no marine terraces have been mapped between ca. 40 and 42 N latitude. In this area models of crustal thickening associated with northward movement of the MTJ at 5.6 cm/yr (Engebretson et al., 1985) predict a wave of high uplift rates propagating northward through the coastal ranges (Zandt and Furlong, 1982). Furlong and Govers (1999) simulated this process using a 2-D numerical model (henceforth, the Mendocino Crustal Conveyor, or MCC model). The MCC model provides a quantitative estimate of both: 1) isostatic uplift due to the northward propagation of crustal thickening and thinning, and 2) zones of uplift and subsidence associated with the northward migration of short-wavelength dynamic topography (Figure 1). Lock et al. (2006) showed that this model is consistent with all the available stratigraphic and geomorphic evidence for deformation in the Northern California Coast Ranges. We further note that the model is consistent with uplift rates inferred from marine terraces at the ends of the model domain (Figure 1). Hence, we suggest that the MCC model uplift field is the best available estimate of millenial-time-scale uplift rates in the region between 40 and 42 N where geomorphic markers of rock uplift are lacking.

Throughout our study area, erosion rates are effectively indistinguishable from uplift rates inferred from marine terraces and predicted by the MCC model. In the central Oregon Coast Range, erosion rates and uplift rates are both near 0.1 mm/yr; this agrees with previous observations that the Oregon Coast Range exhibit a long-term topographic steady-state where uplift is balanced by erosion based on modern sediment-yield data (Reneau and Dietrich, 1991) and cosmogenic ^{10}Be based erosion rates (Heimsath et al., 2001). In the Northern California Coast Ranges, the MCC model predicts large latitudinal variations in uplift rates, with 1) peak uplift rates near 1.5 mm/yr at the latitude of Cape Mendocino, and 2) subsidence, associated with the northward migration of dynamic topography, to the south. Erosion rates in this region range between 0.4-1.1 mm/yr. The highest erosion rates we observed, in the headwaters of the Van Duzen River, occur in the location of highest predicted uplift rates. Most of our study basins in this area span a relatively large range of latitude relative to the short-wavelength variations in uplift rates predicted by the MCC model. The MCC model is two-dimensional and cannot be easily extended to predict the full uplift field in our study basins, so a direct comparison between erosion rates and uplift rates for individual basins is not possible with the available uplift rate estimates. Overall, measured erosion rates and predicted uplift rates are similar in the Northern California Coast Ranges providing no evidence of imbalance between the two.

As the wave of uplift associated with the MTJ moves northward, surface erosion rates have increased to balance uplift. The spatial and temporal scales of the tectonic and erosional processes, however, highlight the significant difficulty of establishing the erosional response to transient tectonic uplift in detail. As noted by Lock et al. (2006), the Northern California Coast Ranges are on average 500 m higher than the Oregon Coast Range (Figure 1); if this increase in elevation results from the transient uplift predicted by the MCC model, then uplift rates must have exceeded erosion rates by an amount, and for a time period, sufficient to explain the modern topographic gradient. The half-width of the MCC model transient uplift is 200 km and the MTJ is migrating to the north at 5.6 cm/yr (Engebretson et al., 1985); thus an average imbalance between uplift and erosion of ~0.15 mm/yr must have been sustained for the period during which the MTJ uplift approached its present position to explain the modern 500-m elevation difference between the Oregon Coast Range and the Northern California Coast Ranges. An imbalance of this magnitude is similar to the uncertainty in our erosion rate measurements, smaller than the expected uncertainty of model assumptions, and cannot be confidently inferred from a comparison of the spatially complex erosion rate and uplift fields available from our measurements, the marine terrace records, and the MCC model uplift field (Figure 1).

Conclusions

Erosion rate measurements from the coastal drainage basins of the Northern California Coast Ranges show the erosional response to the advancing limb of a transient increase in uplift rates accompanying the passage of the MTJ. Erosion rates approximately balance rock uplift rates in the Oregon Coast Range; the relatively high topography of the Northern California Coast Ranges requires that erosion rates have not fully kept pace with increasing uplift rates associated with the northward migration of the MTJ. A comparison of our erosion rate measurements with estimates of uplift rates provides no evidence for such an imbalance, but cannot exclude it given the small magnitude of the expected imbalance and the uncertainties inherent in measuring erosion rates reconstructing uplift rates. This highlights the difficulty of determining whether a landscape is or is not in erosional steady state. However, the relationship between relief and erosion rates in the Northern California Coast Ranges illustrates the role that threshold slope development plays in mediating topographic development in response to a transient tectonic forcing. Within the Oregon Coast Range, erosion rates are correlated with local relief, implying that the balance between uplift and erosion in this region is maintained by changes in hillslope angle and local relief, whereas in the Northern California Coast Ranges, erosion rates become decoupled from local relief, with the mechanically weak lithologies within the Northern California Coast Ranges supporting less relief than other tectonically active mountain ranges where maximum relief has been attained. This transition from sub-threshold to threshold slopes allows relatively rapid erosional accommodation of large gradients in uplift rate with modest physiographic change.

References

Ahnert, F., 1970, Functional relationships between denudation, relief, and uplift in large midlatitude drainage basins: American Journal of Science, v. 268, p. 243–263.

Balco, G., Stone, J.O.H., Lifton, N.A., and Dunai, T.J., 2008, A complete and easily accessible means of calculating surface exposure ages or erosion rates from ^{10}Be and ^{26}Al measurements: Quaternary Geochronology, v. 3, p. 174-195.

Bierman, P.R., Clapp, E.M., Nichols, K., Gillespie, A. and Caffee, M.W., 2001, Using cosmogenic nuclide measurements in sediments to understand background rates of erosion and sediment transport, *in* Harmon, R.S. and Doe, W.M., eds., Landscape Erosion and Evolution Modeling: New York, Kluwer, p. 89-116.

Bierman, P.R., and Nichols, K.K., 2004, Rock to sediment, Slope to sea with 10-Be, Rates of landscape change: Annual Reviews of Earth and Planetary Sciences, v. 32, p. 215-255

Binnie, S.A., Phillips, W.M., Summerfield, M.A., Fifield, L.K., Tectonic uplift, threshold hillslopes, and denudation rates in a developing mountain range: Geology, v. 35, p. 743 – 746.

Blake, M.C., Jayko, A.S., and McLaughlin, R.J., 1985, Tectonostratigraphic terranes of the northern Coast Ranges, California, in Howell, D.G., ed., Tectonostratigraphic terranes of the circum-Pacific region: Houston, Texas, Circum-Pacific Council for Energy and Mineral Resources, p. 159–186.

Brown, W.M., III, and Ritter, J.R., 1971, Sediment transport and turbidity in the Eel River basin, California: U.S. Geological Survey Water-Supply Paper 1986, 70 p.

Burbank, D.W., Leland, J., Fielding, E., Anderson, R.S., Brozovic, N., Reid, M.R., and Duncan, C., 1996, Bedrock incision, rock uplift and threshold hillslopes in the northwestern Himalayas: Nature, v. 379, p. 505–510.

Dott, R. H., Jr., and Bird, K. J., 1979, Sand transport through channels across an Eocene shelf and slope in southwestern Oregon, U.S.A.: Society for Economic Paleontolgists and Mineralogists Special Publication No. 27, p. 327-342.

Engebretson, D.C., A. Cox, and R. G. Gordon, 1985, Relative motion between oceanic and continental plates in the Pacific Basin, Special Paper Geological Society of America, 206, 59 pp.

Ferrier, K.L., Kirchner, J.W., and Finkel, R.C., 2005, Erosion rates over millennial and decadal timescales at Caspar Creek and Redwood Creek, Northern California Coast Ranges: Earth Surface Processes and Landforms, v. 30, p. 1025-1038.

Furlong, K.P. and Govers, R., 1999, Ephemeral crustal thickening at a triple junction: the Mendocino crustal conveyor, Geology, v. 27, p. 127-130.

Granger, D.E., Riebe, C., Kirchner, J., Finkel, R., 2001, Modulation of erosion on steep granitic slopes by boulder armoring, as revealed by cosmogenic ^{26}Al and ^{10}Be. Earth and Planetary Science Letters, v. 186, p. 269-281.

Heimsath, A.M., Dietrich, W.E., Nishiizumi, K., and Finkel, R.C., 2001, Stochastic processes of soil production and transport: Erosion rates, topographic variation and cosmogenic nuclides in the Oregon Coast Range: Earth Surface Processes and Landforms, v. 26, p. 531–552.

Heisinger, B., Lal, D., Jull, A.J.T., Kubik, P., Ivy-Ochs, S., Neumaier, S., Knie, K., Lazarev, V., and Nolte, E., 2002a, Production of selected cosmogenic radionuclides by muons: 1. Fast muons: Earth and Planetary Science Letters, v. 200, p. 345–355.

Heisinger, B., Lal, D., Jull, A.J.T., Kubik, P., Ivy-Ochs, S., Knie, K., and Nolte, E., 2002b, Production of selected cosmogenic radionuclides by muons: 2. Capture of negative muons: Earth and Planetary Science Letters, v. 200, p. 357–369.

Irwin, W.P., 1960, Geologic reconnaissance of the northern Coast Ranges and Klamath Mountains, California: California Division of Mines Bulletin, v. 179, 80 p.

Judson, S. and Ritter, D.F., 1964, Rates of regional denudation in the United States. Journal of Geophysical Research, v. 69 (11), p. 3395-3401.

Kelsey, H.M., Engebretson, D.C., Mitchell, C.E., and Ticknor, R.L., 1994, Topographic form of the Coast Ranges of the Cascadia Margin in relation to coastal uplift rates and plate subduction: Journal of Geophysical Research, v. 99, no. B6, p. 12,245-12,255.

Lock, J., Kelsey, H., Furlong, K., and Woolace, A., 2006, Late Neogene and Quaternary landscape evolution of the Northern California Coast Ranges: Evidence for Mendocino triple junction tectonics: Geological Society of America Bulletin, v. 118, p. 1232 – 1246.

McLaughlin, R.J., Lajoie, K.R., Sorg, D.H., Morrison, S.D., and Wolfe, J.A., 1983, Tectonic uplift of a middle Wisconsin marine platform near the Mendocino triple junction, California: Geology, v. 11, p. 35-39.

McNeill, L.C., Goldfinger, C., Kulm, L.D., Yeats, R.S., 2000. Tectonics of the Neogene Cascadia forearc basin: investigations of a deformed late Miocene unconformity. Geological Society of America Bulletin, v. 112 (8), p. 1209–1224

Merritts, D.J., and Bull, W.B., 1989, Interpreting Quaternary uplift rates at the Mendocino triple junction, northern California, from uplifted marine terraces: Geology, v. 17, p. 1020–1024.

Montgomery, D.R., 2001, Slope distributions, threshold hillslopes, and steady-state topography: American Journal of Science, 301, 432–454.

Montgomery, D.R., and Brandon, M.T., 2002, Topographic controls on erosion rates in tectonically active mountain ranges: Earth and Planetary Science Letters, v. 201, p. 481–489.

Penck, W., 1953, Morphological analysis of landforms (translated by Czech, H., and Boxwell, K. C): London, MacMillan and Company. 429 p.

Reneau, S.L., and Dietrich, W.E., 1991, Erosion rates in the southern Oregon Coast Range: Evidence for an equilibrium between hillslope erosion and sediment yield: Earth Surface Processes and Landforms, v. 16, p. 307–322.

Schmidt, K.M., and Montgomery, D.R., 1995, Limits to relief: Science, v. 270, p. 617–620.

Spatial Climate Analysis Service, 2004, 1971-2000 annual gridded precipitation data, Oregon State University, Corvallis, OR: URL http://www.ocs.oregonstate.edu/prism/.

Stone, J.O.H., Evans, J.M., Fifield, L.K., Allan, G.L., and Cresswell, R.G., 1998. Cosmogenic chlorine-36 production in calcite by muons: Geochimica et Cosmochimica Acta, v. 62, p. 433-454.

Stone J.O. 2000, Air pressure and cosmogenic isotope production. Journal of Geophysical Research, v. 105, p. 23,753-23,759.

Wilson, R.C., 1997, Normalizing rainfall/debris-flow thresholds along the U.S. Pacific Coast for long-term variations in precipitation climate, *in*: Chen, C.L. (ed.) Proceedings first international conference on debris-flow hazards mitigation:

mechanics, prediction, and assessment, 7 – 9 August 1997, Hydraulics Division, American Society of Civil Engineers, San Francisco, CA, p. 32 – 43.

Zandt, G., and Furlong, K. P.,1982, Evolution and thickness of the lithosphere beneath coastal California: Geology, v. 10, p. 376-381.

Figure 1. Erosion rates in Pacific Northwest coastal drainages compared with topography, precipitation and uplift. *Far left:* latitudinal variations in mean (solid) and 95th Percentile (dashed) elevation, computed from SRTM 3-arc second DEM in 0.2° latitude bins extending across the study area shown at right. *Second from left:* 1971-2000 mean annual precipitation (solid), and rainfall intensity (mean annual precipitation normalized by number of rain days) (Spatial Climate Analysis Service, 2004). *Third from left:* erosion rates and uplift rates in study basins. Rectangles show ^{10}Be erosion rate measurements (Table 1 in Data Repository); the height of the rectangles indicates north-south extent of drainage basins, and the width reflects erosion rate uncertainty. The colors reflect different geologic provinces; the Oregon Coast Range (OCR), Klamath Mountains (KM), and Northern California Coast Ranges (NCCR). Blue triangles indicate ^{10}Be erosion rate measurements from other studies. The solid black line is the average uplift rate inferred from terrace elevations between 42°-45° N (Kelsey et al., 1994). The black circles are uplift rates inferred from marine terrace elevations (Merrits and Bull, 1989; McLaughlin et al., 1983). *Far right:* map of study area showing sample locations and corresponding drainage basins.

Figure 2. Erosion rate (E) vs. mean local relief (R_z) of drainage basins within the Klamath Mountains and the Oregon Coast Range (circles) and the Northern California Coast Ranges (squares). We calculated the mean local relief for each watershed by a) calculating local relief for each grid cell as the range of elevations in a 10-km circle surrounding the cell, and b) averaging local relief values for all grid cells in a watershed. The solid line shows $E = 0.2R_z + 0.01$, the relation between relief and erosion rate of Ahnert (1970).

Drainage Basin	Sample Name	Latitude (deg N)	Longitude deg W	Mean Elevation (m asl)	Grain Size (mm)	^{10}Be Conc. atoms/g	+/- atoms/g	Erosion Rate mm/yr	+/- mm/yr	Erosional Timescale Years
Van Duzen	03-INQ-008-VDUS	40.417	123.518	1172	0.25 – 0.5	9.60E+03	1.00E+03	1.060	0.130	559
Eel	03-INQ-015-EEL	40.535	124.156	787	0.25 – 0.5	1.39E+04	7.00E+02	0.579	0.044	1023
Eel	03-INQ-017-EEL	40.568	124.155	772	0.25 – 0.5	1.39E+04	1.70E+03	0.574	0.079	1032
Mad	03-INQ-019-MAD	40.917	124.09	810	0.25 – 0.5	2.06E+04	1.20E+03	0.396	0.032	1495
Redwood	03-INQ-022-RWD	41.289	124.058	573	0.25 – 0.5	1.22E+04	1.10E+03	0.584	0.062	1014
Klamath	03-INQ-024-KLM	41.518	124.031	1153	0.25 – 0.5	3.50E+04	2.00E+03	0.288	0.024	2054
Rogue	03-INQ-027-ROG	42.465	124.369	898	0.25 – 0.5	3.64E+04	1.90E+03	0.239	0.019	2482
Coquille	03-INQ-030-CQL	43.033	124.114	470	0.25 – 0.5	5.10E+04	2.60E+03	0.130	0.010	4568
Umpqua	03-INQ-033-UMP	43.678	123.933	693	0.25 – 0.5	5.94E+04	2.10E+03	0.129	0.009	4608
Smith	03-INQ-035-SMI	43.743	124.037	282	0.25 – 0.5	5.67E+04	2.50E+03	0.104	0.007	5724
Siuslaw	03-INQ-036-SSL	44.051	123.886	303	0.25 – 0.5	6.34E+04	2.40E+03	0.094	0.006	6328
Alsea	03-INQ-037-ALS-O	44.399	123.86	338	0.125–0.5	4.13E+04	1.50E+03	0.150	0.010	3961
Alsea	03-INQ-037-ALS-P	44.399	123.86	338	0.25 – 0.5	4.08E+04	1.70E+03	0.152	0.011	3912
Alsea	03-INQ-037-ALS-Q	44.399	123.86	338	0.5 – 0.85	3.80E+04	1.90E+03	0.163	0.012	3636
Elk	04-NWR-002-ELK	44.603	123.852	245	0.25 – 0.5	3.43E+04	1.00E+03	0.171	0.011	3469
Yaquina	04-NWR-003-YAQ	44.651	123.857	194	0.25 – 0.5	3.39E+04	1.00E+03	0.167	0.010	3540
Salmon	04-NWR-005-SAL	45.023	123.945	381	0.25 – 0.5	4.71E+04	2.50E+03	0.135	0.010	4391
Youngs	04-NWR-015-YNG	46.07	123.786	291	0.25 – 0.5	2.66E+04	1.30E+03	0.230	0.017	2572
Klaskanine	04-NWR-016-NFK	46.094	123.739	268	0.25 – 0.5	1.86E+04	8.00E+02	0.327	0.023	1813

Table 1. Sample locations, Be^{10} concentrations, and drainage basin-scale erosion rates. We separated quartz from grain-size fractions of river sediment by various combinations of density separation and selective etching in HF and NaOH (e.g., Kohl and Nishiizumi, 1992), then extracted Be-10 from quartz using standard methods of HF dissolution and column chromatography (e.g., Stone, 2004). Be^{10}\Be^{9} ratios were measured by accelerator mass spectrometry at the LLNL-CAMS. Be^{10} concentrations are normalized to the standards KNSTD3110 and LLNL3000. Total carrier and process blanks were 4000-8000 atoms Be^{10}, 2-18% of the total number of atoms in the sample. Erosion rate measurements assume a rock density of 2.5 g/cm^{3}.

References

Kohl, C.P., and Nishiizumi, K., 1992, Chemical isolation of quartz for measurement of in-situ-produced cosmogenic nuclides: Geochimica et Cosmochimica Acta, v. 56, p. 3583-3587.

Stone, J., 2004, Extraction of Al and Be from quartz for isotopic analysis. UW Cosmogenic Nuclide Lab Methods and Procedures: URL http://depts.washington.edu/cosmolab/chem.html.

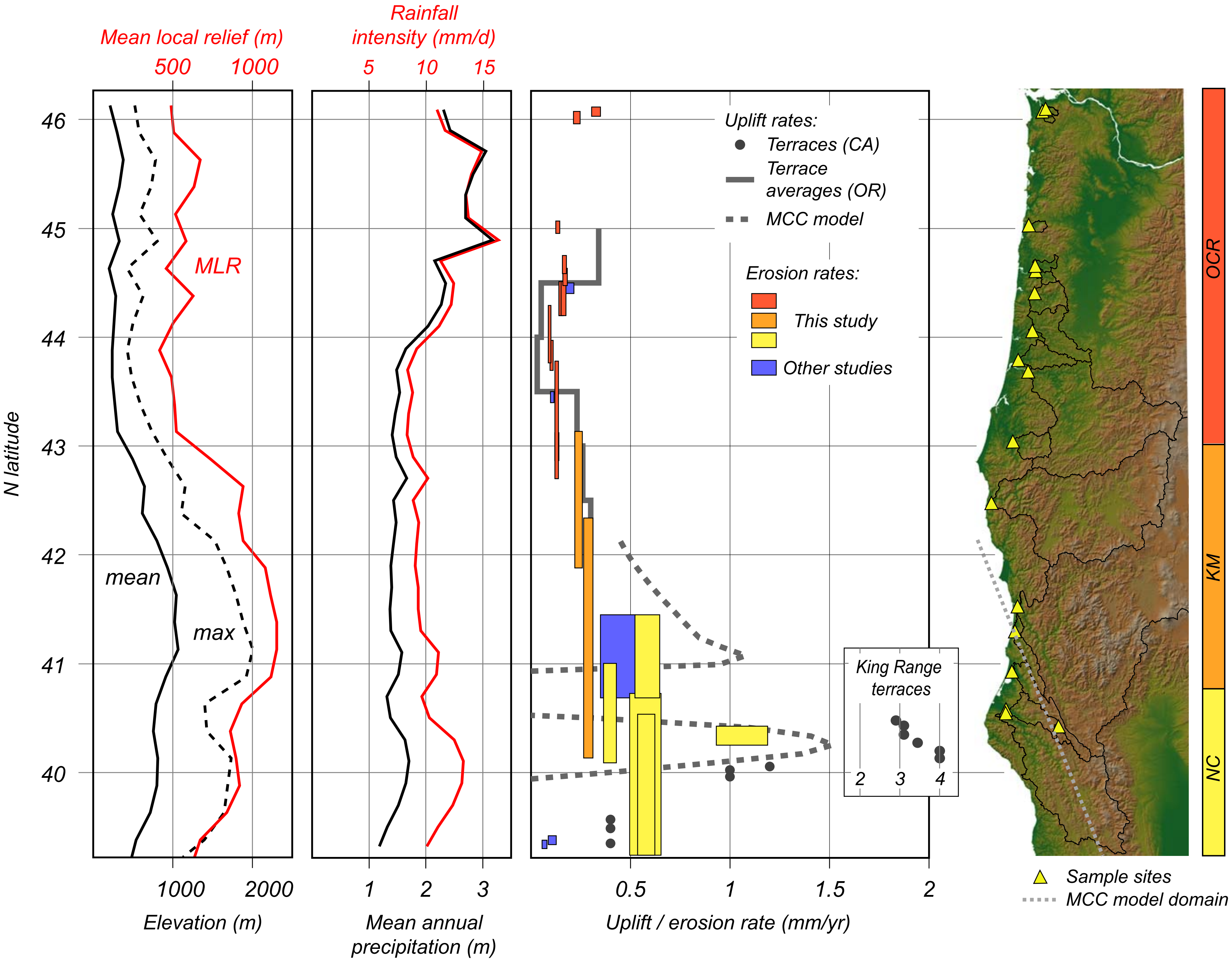
Mean local relief (m)
500
1000
Rainfall intensity (mm/d)
5
10
15
N latitude
46
45
44
43
42
41
40
MLR
mean
max
1000
2000
Elevation (m)
1
2
3
Mean annual precipitation (m)
Uplift rates:
Terraces (CA)
Terrace averages (OR)
MCC model
Erosion rates:
This study
Other studies
King Range terraces
2
3
4
0.5
1
1.5
2
Uplift / erosion rate (mm/yr)
OCR
KM
NC
Sample sites
MCC model domain

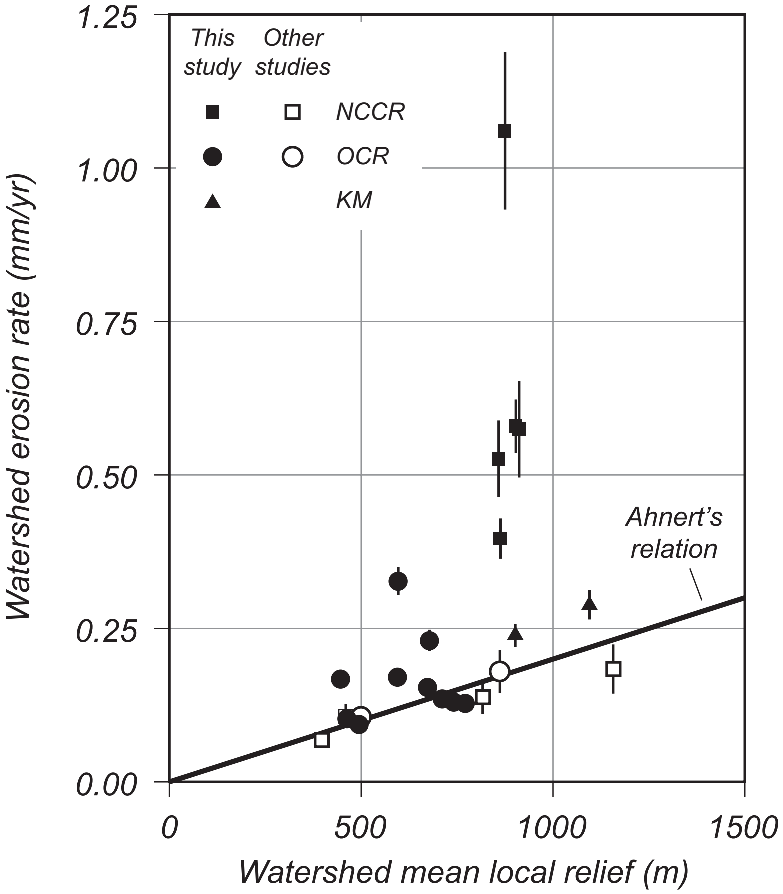
1.25
1.00
0.75
0.50
0.25
0.00
Watershed erosion rate (mm/yr)
This study
Other studies
NCCR
OCR
KM
Ahnert's relation
0
500
1000
1500
Watershed mean local relief (m)